Promoting effect of Mo on the selective hydrogenation of cinnamaldehyde on Rh/SiO_2 catalysts

P. Reyes [a,*], C. Rodríguez [a], G. Pecchi [a] and J.L.G. Fierro [b]

[a] *Departamento de Físico-Química, Facultad de Ciencias Químicas, Universidad de Concepción, Casilla 160-C, Concepción, Chile*
E-mail: preyes@udec.cl

[b] *Instituto de Catálisis y Petroleoquímica, CSIC, Campus Universidad Autónoma, Madrid, Spain*

Received 7 February 2000; accepted 4 July 2000

MoO_3 was added to Rh/SiO_2 catalysts in order to improve both activity and selectivity towards cinnamyl alcohol during the hydrogenation of cinnamaldehyde in the liquid phase. In the present work, four catalysts were studied. Two $Rh–Mo/SiO_2$ catalysts and Rh/SiO_2, Mo/SiO_2 references were prepared by conventional impregnation techniques and characterised by hydrogen chemisorption, X-ray diffraction, transmission electron microscopy, temperature-programmed reduction and X-ray photoelectron spectroscopy. The catalytic behaviour in cinnamaldehyde hydrogenation, after *in situ* reduction treatments in flowing hydrogen at 773 K shows that Mo oxide clearly promotes the hydrogenation of the carbonyl bond. This is attributed to (i) the presence of both MoO_{3-x} and $Rh^{\delta+}$ species which contribute to a polarization of the C=O bond, (ii) the presence of flat surfaces of molybdenum oxides strongly interacting with Rh particles, that provide the appropriate morphology to enhance the selectivity to the unsaturated alcohol, and (iii) the poisoning effect of MoO_x on rhodium species by partial coverage of the metallic particles that produce a decrease in the hydrogenation ability and therefore reduce the formation of the saturated alcohol.

Keywords: catalytic hydrogenation, cinnamaldehyde, rhodium, molybdenum, characterisation

1. Introduction

The selective hydrogenation of carbonyl groups in the presence of olefin groups in α,β unsaturated aldehydes is an important step in the preparation of various fine chemicals used in perfumes, flavorings, and pharmaceuticals [1–3]. From an industrial point of view, the most important product is the unsaturated alcohol and the reaction requires a preferential C=O hydrogenation of the α,β unsaturated aldehydes [4–7]. Thus, selective hydrogenation of the C=O group presents a considerable challenge. Recent research has been devoted to improving the selectivity of heterogeneous supported metal catalysts in these reactions [8–12]. Several research groups have reported catalysts able to selectively reduce certain conjugated aldehydes such as crotonaldehyde and cinnamaldehyde to the corresponding unsaturated alcohols [13–18]. Selectivity towards the allylic alcohol is highly dependent on the nature of the precious metal used as a catalyst [19]. The new design of catalyst with a high selectivity for the reduction of the carbonyl bond, however, usually requires the creation of polar sites that interact with the CO bond and thus lead to its preferential activation.

This may be achieved by using bimetallic catalysts or noble metals supported on reducible oxides. In these cases, the increase in the activity for the hydrogenation of the carbonyl group is attributed to the properties of the bimetallic particles, in which the less noble constituent is not completely reduced under reaction conditions. The presence and the nature of the solvent may also have a significant effect, because it is adsorbed on the catalyst and modifies the surface. The partial and selective coverage of the metal surface by the solvent molecule [20] can be exploited to overcome the production of some unwanted by-products.

The aim of the present study was to determine the effect of Mo on the surface and catalytic properties of Rh/SiO_2 catalysts in the hydrogenation of cinnamaldehyde. The catalysts were characterised by evaluation of specific surface area, H_2 chemisorption, X-ray diffraction, transmission electron microscopy, temperature-programmed reduction, and X-ray photoelectron spectroscopy in order to correlate chemical structures with performance.

2. Experimental

2.1. Preparation

Rh/SiO_2 samples were prepared by impregnation of silica (BASF D11-11, 20–40 mesh, surface area 136 $m^2\,g^{-1}$, pore volume 1.34 $cm^3\,g^{-1}$) with aqueous solutions of $RhCl_3$ (Fluka) and $Mo_7O_{24}(NH_4)_7$ (Aldrich). In all catalysts, the amount of Rh and Mo was kept constant at 1 and 5%, respectively. The Rh–Mo samples were prepared by successive impregnation and coimpregnation. In the former, labelled as Rh–Mo-SI, the silica was impregnated with an aqueous solution containing Rh, dried at 383 K for 12 h, and calcined at 673 K during 2 h. Then, this solid was impregnated with Mo, dried at 383 K and calcined at 673 K. For the coimpregnated catalyst, labelled as Rh–Mo-CI, the

* To whom correspondence should be addressed.

support was impregnated simultaneously with an aqueous solution containing the appropriate amount of $RhCl_3$ and $Mo_7O_{24}(NH_4)_7$. After impregnation, samples were dried at 383 K and calcined at 673 K for 2 h. The samples were reduced *in situ* in hydrogen flow (50 $cm^3\,min^{-1}$) at 773 K for 2 h, before characterisation or catalytic testing. For comparison, two monometallic Rh/SiO_2 and Mo/SiO_2 catalysts were prepared by impregnation using the same procedure previously described.

2.2. Catalysts characterisation

The specific surface area of the catalysts studied were obtained from nitrogen adsorption isotherms at 77 K carried out in a Micromeritics model Gemini 2370 apparatus. Hydrogen chemisorption at 298 K was carried out in a conventional greaseless volumetric adsorption system, equipped with a MKS Baratron 170 M as a sensor of pressure. Before the chemisorption experiments, the samples were reduced *in situ* at 773 K for 2 h and then outgassed for 4 h at the same temperature.

Metal particle size was evaluated by TEM. These studies were performed in a Jeol model JEM-1200 EXII system. The samples were prepared by the extractive replica procedure. XRD studies were carried out in a Rigaku powder diffractometer using nickel-filtered Cu K_α radiation. TPR studies were carried out in a TPD/TPR 2900 Micromeritics system provided with a thermal conductivity detector. The reducing gas was a mixture of 5% H_2/Ar (40 $cm^3\,min^{-1}$) using a heating rate of 10 $K\,min^{-1}$.

XPS spectra were recorded using a VG Escalab 200R spectrometer with a hemispherical analyzer and a monochromatized Mg K_α X-ray source ($h\nu = 1253.6$ eV) operated at 10 mA and 12 kV. The system was provided with a reaction cell to allow pretreatment at high temperatures. The samples were pressed in a hydraulic die to form thin, smooth discs and placed in the cell. The samples were reduced in hydrogen at 773 K, as previously described, and then transported to the analysis chamber without contact with air. Surface Rh/Si and Mo/Si were estimated from the integrated intensities of Rh $3d_{5/2}$, Mo $3d_{5/2}$ and Si 2p lines after background subtraction and corrected by the atomic sensitivity factors [21]. The line of Si 2p at 103.4 eV was used as an internal standard. Rh and Mo peaks were decomposed into several components assuming that the peaks had Gaussian–Lorentzian shapes.

2.3. Catalytic reactions

Catalytic hydrogenation of cinnamaldehyde was carried out at atmospheric pressure in a two-arms glass reactor equipped with magnetic stirring and an electrical heater system with a temperature controller and thermocouples. The catalyst (0.200 g) was added to the reactor and reduced at 773 K for 30 min under a flow of H_2. After cooling to the reaction temperature 323 K, 40 ml of an ethanol solution of cinnamaldehyde 0.5 M was injected into the reactor. The reaction mixture was stirred at 1000 rpm and the reaction was carried out at atmospheric pressure under a flow of H_2 at a rate of 30 $cm^3\,min^{-1}$. A cooling system to prevent ethanol flowing out from the reactor was used. Chemical analysis of the products was performed by a gas chromatography system (IGC 12, INTERSMAT Instruments) equipped with a flame ionization detector. The gas chromatographic column used was 20% SP-2100/0.1% Carbowax 1500 on 100/120 Supelcoport operating at 393 K and using He as carrier.

3. Results and discussion

Table 1 summarizes surface areas obtained from the nitrogen adsorption isotherms at 77 K. From the data in the table it is clear that Rh/SiO_2 shows almost the surface area of the carrier, as expected. Conversely, in all the Mo-containing samples, an important decrease was observed. This can be attributed to a partial coverage of the surface of the support by thin layers of molybdenum oxide, thus leading to a decrease of the mesoporosity of the carrier. The H/Rh atomic ratios and rhodium particle size derived from hydrogen chemisorption measurements at 298 K and TEM are also given in table 1. Previous experiments have shown that Mo/SiO_2 catalysts do not chemisorb H_2 significantly at room temperature [22]. The average particle size was evaluated from the H_2 chemisorption results using the equation $d = 5/S\rho$, where S is the metal surface area and ρ the metal density. The H/Rh values of the Rh–Mo/SiO_2 catalysts are lower than for the monometallic Rh sample. This feature may be attributed to a partial coverage of rhodium particles with highly dispersed MoO_3 but not to a decrease in metal dispersion, as revealed by TEM results. Similar behaviour has been previously reported [22–24] in Rh–Mo supported catalysts. In fact, the TEM results suggest an increase in rhodium dispersion in the Rh–Mo catalysts compared with the monometallic Rh/SiO_2 (figure 1 (a) and (b)). This behaviour may be accounted for in terms of the zero-point charge (ZPC) of the support [25]. The pH of the impregnation solution in the preparation of the Rh monometallic catalyst was approximately 3, as compared with the ZPC, 1–2 of the support, implying that the precursor–support interaction is rather weak, allowing a partial agglomeration of the precursor and hence limiting a high metal dispersion. In the Rh–Mo-SI sample, after molybdenum oxide deposition on silica, the ZPC of the carrier shifted to higher values 3–4, allowing a better interaction with the cationic precur-

Table 1
Surface area, H/Rh and rhodium particle size obtained from chemisorption and TEM for Rh–Mo/SiO_2 catalysts.

Catalyst	S_{BET} ($m^2\,g^{-1}$)	H/Rh	Particle size, d (nm)	
			CHEM	TEM
Rh	130	0.52	1.7	1.8
Rh–Mo-SI	70	0.34	2.9	1.3
Rh–Mo-CI	72	0.31	2.7	1.2
Mo	76	–	–	–

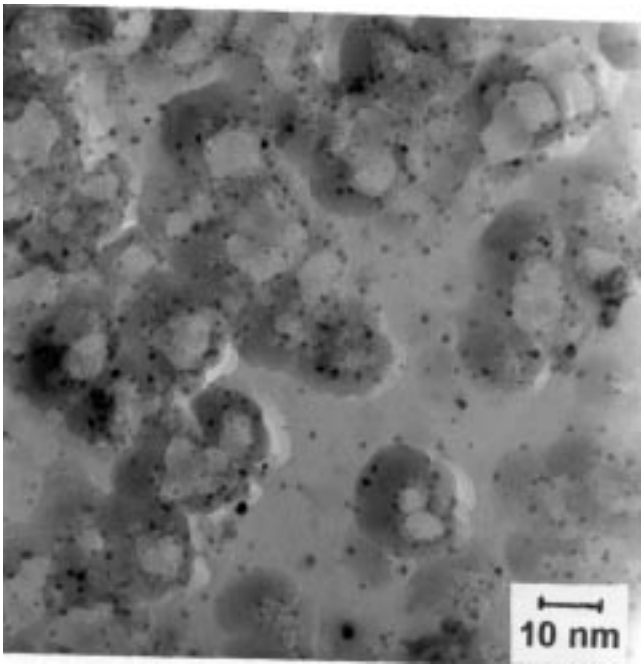

(a)

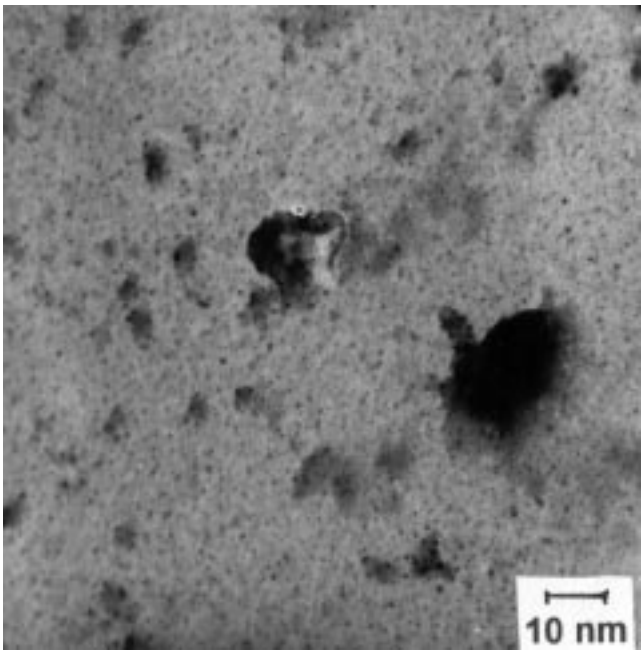

(b)

Figure 1. TEM micrographs of (a) Rh/SiO_2 and (b) $Rh–Mo/SiO_2$ catalysts.

sor of rhodium and, therefore, a higher metal dispersion should be obtained. A similar type of behaviour may be expected for the Rh–Mo catalysts prepared by coimpregnation since the molybdenum precursor is first adsorbed onto the support due to electrostatic considerations. On the basis of these arguments, it is likely that the rhodium species remain mainly deposited on the molybdenum oxide than on silica in these Rh–Mo catalysts.

The XRD patterns of the studied catalysts are shown in figure 2. No lines attributed to rhodium can be seen in

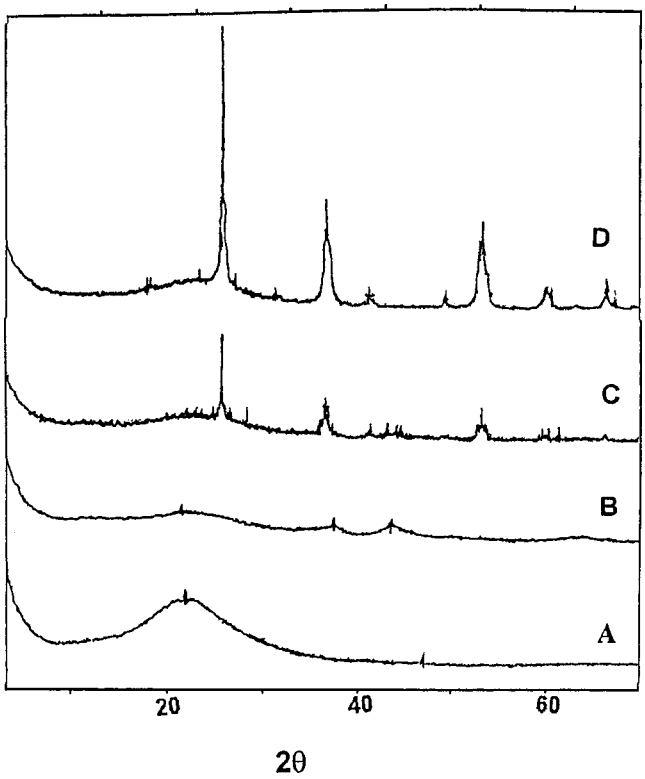

Figure 2. X-ray diffraction patterns of $Rh–Mo/SiO_2$ catalysts: (A) Rh, (B) Rh–Mo-SI, (C) Rh–Mo-CI and (D) Mo.

any of the catalysts, confirming the high dispersion of the metal. With regard to the molybdenum component, lines attributed to crystalline molybdenum trioxide are observed in the Mo/SiO_2 sample. The MoO_3 particle size evaluated by the Debye–Scherrer equation, indicates a value of 6.0 nm. A lower degree of crystallinity of MoO_3 is observed in the Rh–Mo catalysts prepared by coimpregnation (3.5 nm), whereas the catalyst sample obtained by successive impregnation (molybdenum first, then rhodium) is almost amorphous. This result is in agreement with previous findings indicating the redispersion of molybdenum species in the presence of a metal [26].

Figure 3 shows TPR profiles of Rh–Mo catalysts. In the calcined Rh/SiO_2 sample, a single peak centred at 400 K corresponding to the reduction to Rh_2O_3 can be observed. Mo/SiO_2 only exhibits a reduction peak at higher temperatures. The reduction starts at 763 K showing a peak centered at 840 K. In the bimetallic Rh–Mo samples two peaks were observed. The one at lower temperatures (439 and 465 K for Rh–Mo-SI and Rh–Mo-CI, respectively) corresponds to the reduction of rhodium oxide and to a partial reduction of MoO_3 in intimate contact with rhodium, which induces the reduction of molybdenum oxide by hydrogen spillover. Hydrogen consumption is approximately six-fold higher than the theoretical one required for the reduction of the rhodium oxide, indicating a reduction of MoO_3 to MoO_2 to a considerable extent. The peak at higher temperatures, close to 673 K may be assigned to the reduction of isolated patches of MoO_x species.

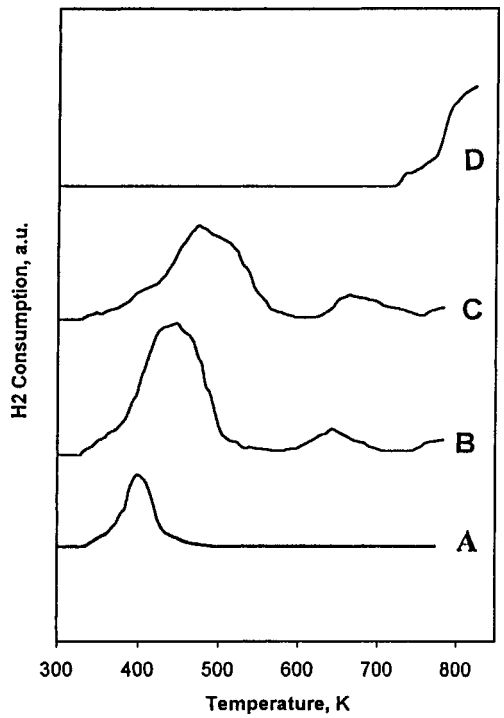

Figure 3. Temperature-programmed reduction profiles of Rh–Mo/SiO_2 catalysts: (A) Rh, (B) Rh–Mo-SI, (C) Rh–Mo-CI and (D) Mo.

In figure 4 (a) and (b), the Rh 3d and Mo 3d core level spectra, respectively, of the reduced catalysts are given. The BE of the Rh $3d_{5/2}$ peak at ca. 307.2 eV for Rh^0 is observed in the monometallic Rh/SiO_2 whereas in those Rh–Mo catalysts a slight shift towards higher BE values suggests the presence of $Rh^{\delta+}$ species. In fact, Rh 3d peak decomposition leads to approximately 15–20% of these partially oxidized species whose origin comes from oxygen transferred from MoO_x species. The Mo 3d profile for Mo/SiO_2 is the expected for MoO_3 species. In those corresponding to Rh–Mo catalysts the profiles show significant changes due to the presence of reduced species. In fact, curve fitting of the experimental spectra indicates reduced molybdenum species, Mo^{4+}, in a proportion close to 70%. The fitting into Mo^{6+} and Mo^{4+} oxides is not completely satisfactory being also possible to have a proportion of Mo^{5+} species. These results are in good agreement with those coming from the TPR experiments, indicating that metallic Rh catalyzes the reduction of MoO_3. Table 2 gives the Rh/Si and Mo/Si atomic surface ratios obtained from XPS. The Rh/Si is lower in the Rh/SiO_2 compared with the Rh–Mo/SiO_2 catalysts. This may be a consequence of the higher rhodium dispersion in the latter, or alternatively could be due to the increase in the Rh/Si ratio in the bimetallic samples, resulting by coverage of the SiO_2 sur-

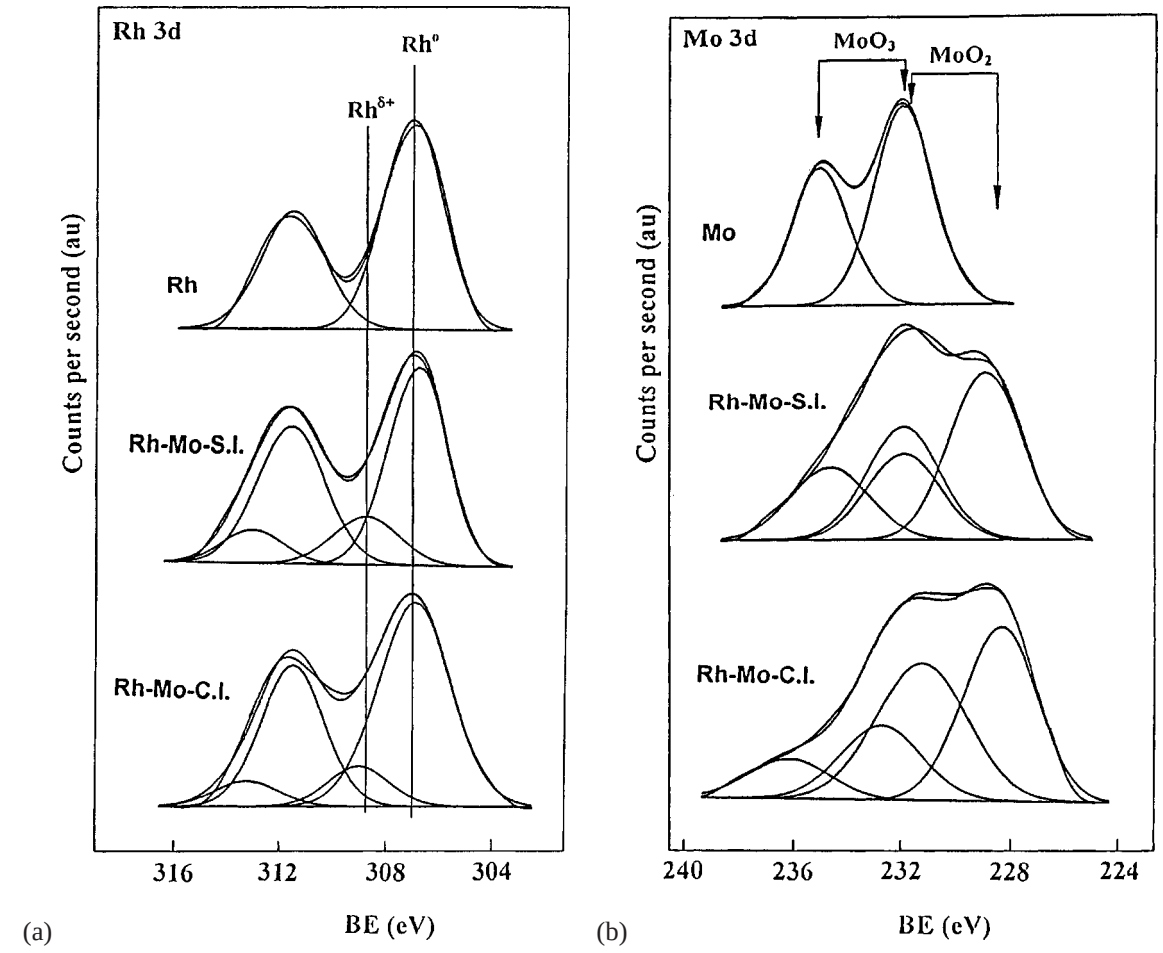

Figure 4. XP spectra of (a) Rh $3d_{5/2}$ and (b) Mo $3d_{5/2}$ core levels of different prereduced Rh–Mo/SiO_2 catalysts.

Table 2
Binding energies (eV) of Rh $3d_{5/2}$ and Mo $3d_{5/2}$ core levels and Rh/Si, Mo/Si, and Rh/(Mo + Si) atomic surface ratios obtained from XPS data for Rh–Mo/SiO_2 catalysts.

Catalyst	BE (eV)		Rh/Si	Mo/Si	Rh/(Si + Mo)
	Rh $3d_{5/2}$	Mo $3d_{5/2}$	(at/at)	(at/at)	(at/at)
Rh	307.3	–	0.0022	–	0.0022
Rh–Mo-SI	307.1(85)	229.0(73)	0.0035	0.106	0.0032
	309.0(15)	232.4(27)			
Rh–Mo-CI	307.1(81)	292.4(64)	0.0030	0.054	0.0029
	309.0(19)	232.2(36)			
Mo	–	232.0	–	0.090	–

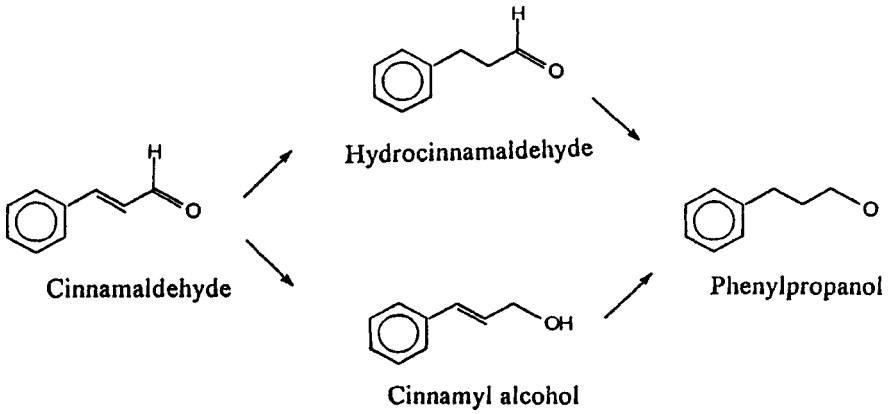

Figure 5. Reaction pathway for cinnamaldehyde hydrogenation.

Table 3
Initial reaction rate, selectivity towards cinnamyl alcohol and activation energy for hydrogenation of cinnamaldehyde at 323 K on Rh–Mo/SiO_2 catalysts.

Catalyst	r (μmol s^{-1} g-cat^{-1})	Selectivity COL (%)	Activation energy (kJ mol^{-1})
Rh	2.8	70	19.5
Rh–Mo-SI	4.4	98	19.2
Rh–Mo-CI	11.1	97	20.2
Mo	1.0	48	18.0

face by MoO_x species and hence leading to a decrease in Si atoms; the Rh/Si ratio should therefore increase. In order to rule out this possibility. Table 2 also gives the Rh/(Si+Mo) atomic ratio. As can be seen, the Rh surface composition increases in the bimetallic catalysts indicating higher metal dispersion and consequently smaller metal particle size, in agreement with TEM results.

The cinnamaldehyde hydrogenation was studied at 313 and 323 K and atmospheric pressure and the obtained products were cinnamyl alcohol (COL), hydrocinnamaldehyde (HCAL) and phenylpropanol (PhPOL). No formation of other by-products was detected. Figure 5 shows a reaction pathway for the cinnamaldehyde hydrogenation. Significant differences in conversion levels were found for the studied catalysts. Activity increases in the following order: Mo < Rh < Rh–Mo-SI < Rh–Mo-CI. A similar trend was observed at 313 K, but showing lower conversion levels and small changes in selectivity. Table 3 summarizes the initial reaction rate, the selectivity towards cinnamyl alcohol (COL) and the activation energy in the cinnamaldehyde (CAL) hydrogenation at 323 K.

Product distribution was found to depend on the catalyst used. On the Mo/SiO_2 sample, the main products were PhPOL and COL. In the Rh and Rh–Mo/SiO_2 catalysts the main product is the COL, with a small contribution of HCAL for the former and PhPOL for Rh–Mo catalysts. Eventhough S_{COL} is very high, the effect of Mo is to activate the C=O bond rendering the hydrogen transfer from adjacent Rh sites easier. The activating effect of Mo can be ascribed to Mo ions present on the catalytic surface that polarize the carbonyl group since it is generally accepted that the electropositive metal or ionic species ($M^{\delta+}$) polarizes the C=O bond, making it more reactive towards the attack by hydrogen [16,27]. Molybdenum oxide can also produce a partial oxidation of rhodium, generating $Rh^{\delta+}$ species (which are also responsible for C=O bond polarization). Additionally, since molybdenum is present in the form of an oxide – MoO_x, which usually shows a flat surface – and since small rhodium species are in intimate contact with these species, the catalyst surface offers an appropriate morphology. It should be borne in mind that geometric effects, depending on both the morphology of the metal particles and the steric configuration of α, β unsaturated aldehydes molecules, may have a significant impact on selectivity. It is expected that larger metal particles would give a higher selectivity to COL than smaller ones [15,28]. In the Mo/SiO_2 catalysts, the morphology is the appropriate but it does not have an important hydrogenation capacity,

accounting for its low activity. On the other hand, the Rh/SiO_2 catalyst displays a decrease in selectivity to COL with time. This behaviour may be the result of a strong adsorption of the organic substrate onto some highly unsaturated sites of the metal particle, which limits the access of new reactant molecules to the active site inducing the metal–reactant interaction by the carbonyl bond.

As it is well known, metal particles larger than 2–3 nm (at least compared to the dimension of the cinnamaldehyde molecule) are more selective than smaller particles. This may be attributed to the different steric constraints of the CAL when it is adsorbed onto a flat or curved (stepped) metal surface. The observed improvement in the selectivity to COL on $Rh–Mo/SiO_2$ catalysts having small Rh particles may be attributed to a promotional effect of Mo due to the creation of mixed $Rh^{\delta+}$–MoO_x sites which activates the C=O bond with a result of better reactivity and selectivity to COL.

4. Conclusions

The activity and selectivity of Rh supported catalyst was modified by the presence of molybdenum oxides. The activity and selectivity to cinnamyl alcohol was enhanced in Rh–Mo catalysts as compared with the monometallic counterparts. The observed improvement in the selectivity to COL on $Rh–Mo/SiO_2$ catalysts having small Rh particles may be attributed to a promotional effect of Mo due to the creation of mixed $Rh^{\delta+}$–MoO_x sites which activates the C=O bond with a result of better reactivity and selectivity to COL.

It was found that these types of behaviour may due to the followings facts: (i) rhodium induces a reduction of MoO_3 to MoO_x species and (ii) molybdenum oxide can also produce a partial oxidation of rhodium, generating $Rh^{\delta+}$ species in intimate contact with MoO_x, which are responsible for C=O bond polarisation,

Acknowledgement

The authors thank CONICYT (FONDECYT Grants 1980345 and 2000116 and CSIC-CONICYT Collaboration Programme) for financial support.

References

[1] Z. Poltarzewski, S. Galvagno, R. Pietropaolo and P. Staiti, J. Catal. 102 (1986) 190.
[2] L. Cerventy and V. Ruzicka, Catal. Rev. Sci. Eng. 24 (1982) 503.
[3] E. Farnetti, M. Pesce, J. Kaspar, R. Spogliarich and M. Graziani, J. Chem. Soc. Chem. Commun. (1986) 746.
[4] G. Neri, L. Mercadante, A. Donato, A. Visco and S. Galvano, Catal. Lett. 29 (1994) 379.
[5] J.L. Margitfalvi, A. Tompos, I. Kolosova and J. Valyon, J. Catal. 174 (1998) 246.
[6] K. Bauer and D. Garbe, in: *Common Fragance and Flavour Materials* (VCH, New York, 1985).
[7] C.G. Raab, M. English, T.B.L.W. Marinelli and J.A. Lercher, in: *Proc. 3rd Int. Symp. Fine Chemicals Catal.*, Poitiers, 1993, eds. M. Guisnet, J. Barbier, J. Barrault, C. Bouchoule, D.D. Duprez, G. Pérot and C. Montassier (Elsevier, Amsterdam, 1993) p. 211.
[8] D.G. Blackmond, R. Oukaci, B. Blanc and P. Gallezot, J. Catal. 131 (1991) 401.
[9] A.M. Vannice and B. Sen, J. Catal. 65 (1989) 115.
[10] D. Goupil, P. Fouilloux and R. Maurel, React. Kinet. Catal. Lett. 35 (1987) 185.
[11] R. Hubaut, M. Daage and J.P. Bonnelle, Appl. Catal. 22 (1986) 231.
[12] P. Beccat, J.C. Bertolini, Y. Gauthier, J. Massardier and R. Ruiz, J. Catal. 126 (1990) 451.
[13] S. Galvagno, Z. Poltarzewsky, A. Donato, G. Neri and R. Pietropaolo, J. Chem. Soc. Chem. Commun. (1986) 1729.
[14] M. Shibata, N. Kawata, T. Matsumoto and H. Kimura, J. Chem. Soc. Chem. Commun. (1988) 99.
[15] A. Giroir-Fendler, D. Richard and P. Gallezot, Catal. Lett. 5 (1990) 175.
[16] M.A. Aramendía, V. Borau, C. Jimenez, J.M. Marinas, A. Porras and F.J. Urbano, J. Catal. 172 (1997) 46.
[17] F. Coloma, A. Sepulveda-Escribano, J.L.G. Fierro and F. Rodríguez-Reinoso, Appl. Catal. A 136 (1996) 231.
[18] P. Fouilloux, Stud. Surf. Sci. Catal. 41 (1988) 123.
[19] A. Giroir-Fendler, D. Richard and P. Gallezot, Stud. Surf. Sci. Catal. 41 (1988) 171.
[20] V. Ponec, Appl. Catal. A 149 (1997) 27.
[21] C.D. Wagner, L.E. Davis, M.V. Zeller, J.A. Taylor, R.H. Raymond and L.H. Gale, Surf. Interface Anal. 3 (1981) 211.
[22] P. Reyes, J. Fernández, I. Concha, G. Pecchi, M. López Granados and J.L.G. Fierro, Catal. Lett. 34 (1995) 331.
[23] D.A. Storm, F.P. Mertens, M.C. Cataldo and E.C. DeCanio, J. Catal. 141 (1993) 478.
[24] J.Y. Sher, T. Matsuzaki, T. Hanaoka, K. Takeuchi and Y. Sugi, Catal. Lett. 28 (1994) 329.
[25] J.P. Brunelle, Pure Appl. Chem. 50 (1978) 1211.
[26] C.V. Cáceres, J.L.G. Fierro, M.N. Blanco and H.J. Thomas, Appl. Catal. 10 (1984) 333.
[27] B. Coq, P.S. Kumhar, C. Moreau anf F. Figueras, J. Phys. Chem. 98 (1994) 10180.
[28] Y. Nitta, K. Ueno and T. Imanaka, Appl. Catal. 56 (1989) 57.